Pilot tests of FasTR method for locating transient faults in medium voltage underground power networks

Moussa Kafal, Nicolas Gregis, Jaume Benoit, Nicolas Ravot, Clara Lagomarsini, Gabriel Gobat

Pilot Tests of FasTR Method for Locating Transient Faults in Medium Voltage Underground Power Networks

Some of the authors of this publication are also working on these related projects:

FLOW-CAM View project

Advances in reflectometry techniques for complex transmission line network diagnosis View project

Pilot Tests of FasTR Method for Locating Transient Faults in Medium Voltage Underground Power Networks

Moussa Kafal, *Member, IEEE*, Nicolas Grégis, Jaume Benoit, Nicolas Ravot, Clara Lagomarsini, and Gabriel Gobat

Abstract—This paper presents the results of pilot tests performed on a real medium voltage (MV) underground network in Switzerland with the aim of assessing the performance of a fault location system. The deployed fault location platform is based on a very sensitive and precise acquisition system which is capable of capturing perturbations or events on a dedicated portion of a given MV network. Thanks to a post processing algorithm based on the tenets of time reversal theory, FasTR method, an accurate localization of relevant events can be worked. Due to the fact that each acquisition system shares a clock reference based on a GPS antenna, the localization accuracy is within tens of meters. To the best of the Authors knowledge, this is the first time that the FasTR-based fault location technique is validated through live tests. The pilot network is a three branch system part of live radial MV distribution feeder consisting of a total of 2.6 km long underground three-phase cables. The branched lines are composed of coaxial cables of different types. The tests involve solid- and resistive-type single-phase-to-ground fault occurrences triggered along one of the laterals when the network is operational. The obtained results demonstrated the capacity of an on-deck portable system to make an on-line accurate detection of transient faults in a complex network.

Index Terms—Electromagnetic time reversal, fault location, optimization techniques, power system faults, power system transients, power system protection, pilot test.

I. INTRODUCTION

THE global electrical energy sector is undergoing radical changes in every segment of the power industry, from generation to supply. Ambitious policy goals set at the universal level to enhance the competitiveness, security and sustainability of energy systems have called for major changes in the regulatory, technological, and market structure fields. Particularly, the issue of undergrounding overhead lines has been forming a pivotal anchor of interest for the energy market worldwide. When lifetime costs, environmental compelling factors, urban space problems, maintenance as well as other advantages of underground cables are taken into account, these latter can be considered as a feasible solution especially for increased security of supply in critical sections of electricity networks. Within this context, medium voltage cables (MV) present a cornerstone of power distribution systems, providing the electricity connections that deliver electrical energy to its ultimate point of consumption. In particular, underground MV cables have been offering an affordable and secure energy allocation for distribution networks by ensuring uninterrupted power supply that is hitherto uncommon in overhead systems. Remarkably, some countries as Netherlands have fully de-ployed underground cables for its MV distribution networks [1], while others are gradually shifting.

MV underground cables are qualified by various manufacturers to provide a specified life of anywhere from 20 to 30 years of continued service in optimal environmental and operating conditions [2]. However they are still exposed to a number of detrimental factors, from water exposure, ionized soil and such thus exposing them to deterioration with time leading to incipient, self-clearing faults prior to permanent failure. Notwithstanding their reliability, underground cables provide limited and hard access which in turn complicates and increases the costs of the procedures needed for their inspection. While, more than 90 % of the outages experienced by customers are due to faults in the latter [3], non-destructive fault detection and location methods became vitally important as an early warning approach [4].

A large number of methods have been introduced in the past few decades for fault location in power grids, among which those based on traveling waves facilitated fault location and reduced costs [5]–[8]. The major drawback of such methods is that they require complex signal processing techniques and large bandwidth measuring systems. To cope with such limitations, considerable attention has been recently devoted to use the concept of time reversal (TR) focusing [9] for fault diagnosis in transmission lines [10]–[12]. In this respect, electromagnetic TR (EMTR) as proposed in [13] is considered the first embodiment; it has proven an ability to locate faults from the transient signals they generate, as measured from a single or multiple probes. Its performance has been shown to

depend on what kind of metrics are used, e.g., by monitoring the maximum focused energy or peak amplitude [14]–[16]. EMTR has been validated on both reduced- and large-scale experimental setups [13], [17], and on an operational real MV distribution network [18]. Nevertheless, fault identification entailed cumbersome post-processing simulations and achieving high location accuracy has shown to require a considerable computation time.

Within the same context, a recent proposal for fault location in power grids is FasTR [19], a method also inspired from the idea of TR focusing. Thanks to a simplified analytical model that computes the voltage (or the current) at any position and any instant of the network under test (NUT), FasTR gets rid of the ponderous simulation stage endured by EMTR [19]. It has proven an ability of locating faults from their emitted transient signals recorded with precision from probes placed at distant locations of the tested network, by virtue to an accurate shared time synchronization system. FasTR is shown to extend the possibilities of diagnosing MV networks on a larger scale by placing sensors on well chosen nodes of the network for continuous monitoring.

Up-to-the-date, FasTR-based fault location method has never been tested by making use of live power networks affected by manually triggered real events. Therein, this paper presents the results of a pilot test performed on an operational MV underground distribution network in Switzerland. Indeed, to the best of the Authors' knowledge, this is the first time that the FasTR algorithm is validated on a realistic power network under normal operating conditions and its performance is evaluated with respect to faults of different types. This pilot test itself represents an original contribution, especially in view of the following observations.

- The NUT presents a complex topology with several laterals forming up numerous subnetworks. It also features non-homogeneity, i.e, segments composed of cables of different types. Notwithstanding, using distributed sensing units and a calibration process, FasTR is still capable of locating with a considerable accuracy occurring events.
- The developed on-the-shelf system is compact and portable so that to be easily transported and implemented on any network of interest. Particularly, the adopted sensors are contactless inductive couplers permitting an effortless installation.
- Measured data corresponding to detected events, are transferred to a remote server, thanks to a realized communication system and protocol. The server platform comprises a database for saving the recorded events and a computer unit accommodating the FasTR algorithm for processing. The obtained results are saved and communicated with local operators for quick intervention.
- The fault-location platform completes a testing cycle starting from the moment a fault occurs to the instant the fault-related information is retrieved and broadcasted in a handful minutes. A remarkable unique feature in the domain of fault location in power networks.

The structure of the paper is organized as follows. Section II recalls the basic principles of FasTR method and presents its corresponding algorithm. In Section. III, the designed fault location system is described by introducing its architecture as well as detailing each of the block functions which include the sensing units, the data acquisition system, the communication tool and finally the fault location platform comprising the database and the FasTR processing unit. This is followed by Section. IV, where the on-site implementation of the fault location global setup is demonstrated. The pilot network investigated in our study is illustrated in Section V where the tested MV underground radial network is first elucidated, and the fault generation system with its position reasoning is introduced. The triggered faults, including their amplitude and spectral features, are clarified in Section VI, and the fault related information (position and location) retrieved after applying the FasTR processing is analyzed. Section VII reports a performance analysis of the obtained results covering several aspects not limited to the location accuracy and network coverage. Finally, Section VIII concludes this paper by addressing the final remarks on the performance of the proposed method and proposes some perspectives.

II. FasTR IN A NUTSHELL

Thanks to the TR invariance of the transmission-line equations and the inherent spatial focusing property of the TR invariant system, FasTR has emerged as a promising technique for detecting and locating faults in power systems [19]. With a limited knowledge of the tested network and a moderate need for computing resources, FasTR follows a similar analogy to EMTR based methods but uses a different post-processing approach for locating the fault. Meanwhile, both techniques share a two phases foundation composed of: the forward propagation phase (FPP) and the backward propagation phase (BPP). In the FPP, the fault originating transient (FOT), which is a high frequency, short duration signal resulting from a sudden change affecting the network, is recorded using probes on a single or multiple observation points. Subsequently, in the BPP of EMTR methods, time-reversed versions of the probe-recorded FOTs, are injected in numerical models of the NUT, where different candidate fault positions x_c are tested. EMTR estimates the actual fault position by identifying the position x_c with the maximum signal energy or amplitude depending on the norm used [13], [14]. However, this endures cumbersome simulations as the BPP shall be repeated for all candidate positions. FasTR, instead, proposes an alternative technique to get rid of the heavy simulation stage by optimizing a function representative of the energy propagating along the network, thanks to an in-house analytical model expressing the voltage (or current) at any position x and any instant t. Accordingly, estimating the fault's location is accomplished by the following steps:

1) the FOT is measured using probes coupled at predefined nodes of the NUT;
2) the recorded measurements are time-reversed and numerically re-injected into a simulation model of the network;
3) a cost function $F(x, t)$ is constructed which aims at estimating the signal corresponding to the superposition

of the back-propagated TR signals, at each instant t and position x of a point in the network; $F(x,t)$ is illustrated as

$$ F(x,t) = \sum_{e=1}^{n_r} \left[Sr_e \left(x, t - \frac{d(x, x_e)}{v_{b_i}} \right) \times \frac{e^{\alpha_{b_i} d(x, x_e)}}{C_e^{b_i}} \right] $$

ω_b is the set of points of branch b_i of the NUT, T_{rec} and T_{max} are respectively the total recording time of the signals and the time taken by a signal to travel the maximum distance present in the network. n_r is the total number of extremities employing measurements devices. Notably, n_r is at least two and no more than the number of ends of the network. Sr_e is the time-reversed version of the signal measured at extremity e with ($e \in [1, n_r]$), while $d(x, x_e)$ is the distance between any point of the network, of coordinate x, and an end of the NUT of coordinate x_e. On the other hand, v_{b_i} is the velocity of signal propagation along branch b_i, thus $d(x, x_e)/v_{b_i}$ is the time taken for the signal to travel the distance $d(x, x_e)$. α_{b_i} is the attenuation factor of waves propagating at each branch b_i, while $C_e^{b_i}$ is the aggregated transmission coefficient between the extremity e and branch b_i. For networks composed of several junctions, $C_e^{b_i}$ is obtained by multiplying the transmission coefficients associated with each junction crossed.

4) having computed $F(x,t)$, a searching mechanism for detecting its extremum is launched, thanks to a wide selection of optimization algorithms.

We adopted in our study the genetic algorithm, a dynamic random-search oriented optimization approach, that has proven efficacy in solving inverse problems [20]. The extremum's coordinates (x_f, t_f) provide the estimated position of the fault through x_f, and makes it possible to determine the instant at which the FOT has occurred via t_f.

III. FAULT LOCATION GLOBAL SETUP

The on-line real-time fault monitoring framework is based on two main systems: a measurement system composed of distributed high-speed sensing devices to capture fault-related events with a communication tool between sensors, and an elaborate platform to perform the FasTR fault location process. The high-precision measurement devices are firstly installed on distant points of the tested MV network which are responsible for continuously monitoring signals over one of the phases in operation. Once a FOT occurs, the corresponding voltage and current surge that propagate along the network is recorded by the sensing units which share the same time reference, thanks to their precise synchronization. Particularly, this is intended to timestamp their moment of arrival at the level of each of the sensors. Through the communication network, the recorded data affiliated with their respective timestamps are transferred from the measurement devices to a server. Subsequently, a built-in platform implementing the FasTR algorithm post-processes the measured data to mark the defected segment and locate the position and time at which the FOT has burst.
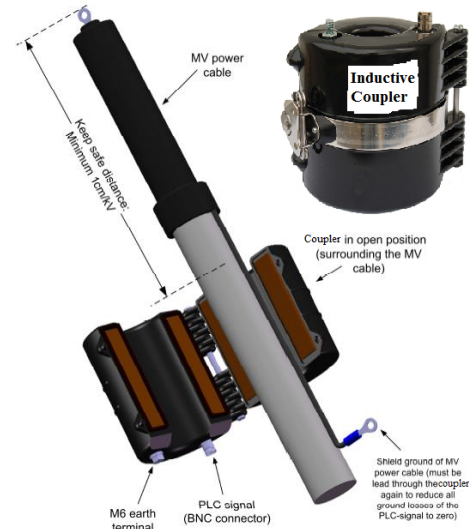

Fig. 1: An installation guide diagram of the inductive coupler (upper right) which is considered as the sensing unit to acquire the FOT on the tested MV networks.

A. The Measurement System

The measurement system is composed of two main elements: the sensing unit, and the data acquisition system which embeds a synchronization module.

1) Sensing Unit: The selection process of the sensing unit has to consider several factors particularly the sensor's frequency bandwidth that shall be capable of covering the FOT's frequency spectrum. Likewise, special attention has to be put on the sensor's ability to perfectly isolate the high voltage low frequency component on MV networks so as not to damage the connected equipment. In our tests, we adopted the inductive coupler shown in Fig. 1. With a compact size (height=117 mm and width=106 mm), a high insulation at voltages up to 4.7 kV thus ensuring a good electrical safety, an easy installation as shown in Fig. 1, a rated current of 300 A, and a frequency range of 30-500 KHz, the adopted coupler provided a good match with our specifications for acquiring FOTs. To do so, the coupler is capable of extracting the high-frequency transients that are superimposed to the network's steady state frequency component (e.g., 50 Hz). Subsequently, the acquired FOTs are transferred to the acquisition block where a threshold-triggering criterion is implemented so as to decide whether a fault-related event has eventually occurred or not. More importantly, since the switching frequencies of the measured fault voltage signals in the tested cases were above 30 KHz and well below 500 KHz, the selected coupler has sufficient bandwidth to isolate and capture them.

2) Data Acquisition System: Having coupled the sensing unit to the tested cable (pre-planned phase to test) at the NUT's observation points, each of the inductive couplers is then connected to an acquisition system via a 50-Ohm coaxial cable. The acquisition system is meant to acquire the measured FOTs from the defected MV power network that will be further sent to a server where the FasTR processing is applied. The acquisition system is assembled by National Instrument (NI) products and is composed of four main modules consisting
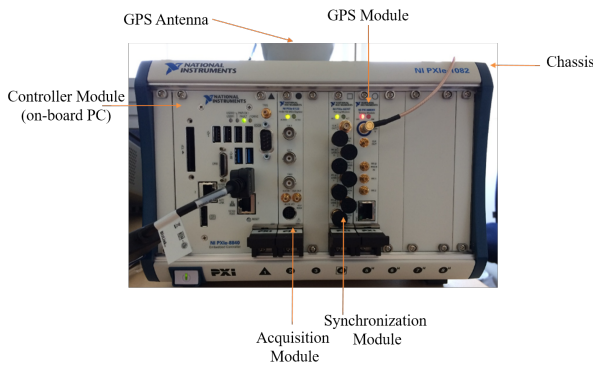
Fig. 2: The National Instrument built data acquisition system embedding different modules.

of a controller module (on-board PC), an acquisition module, a GPS module (including the antenna) that is coupled to a module allowing the clock synchronization of all the other installed modules in the chassis.

The controller module is a high performance Intel processor ideal for modular instrumentation and processor time consuming data acquisition applications, with a system bandwidth up to 8 GB/s. On the other hand, the acquisition module is a high resolution oscilloscope that allows continuous data transfer at the speed of 400 MB/s to the PC memory. With a sampling frequency of 100 MS/s real-time and up to 2.0 GS/s equivalent-time, the considered module is perfectly suited for sampling the high frequency acquired FOTs. Particularly, using a 100 MS/s sample rate allows us to set one point every 10 ns which is at least two orders of magnitude shorter than the expected rise time of the fault.

The GPS and clock synchronization module enables timing and synchronization features capable of synchronizing PXI and PXI Express systems using the GPS, IEEE 1588 [21], IRIG-B or PPS protocols [22]. In our application, we use the GPS protocol. It can generate triggers and clock signals at programmable future times, and time stamp input events, using synchronized system time.

Each acquisition system is deployed on distant predefined observation points on the tested large MV power network. To reveal the occurrence of an event, an adequate triggering system capable of detecting high-frequency FOTs is necessary. As mentioned earlier in sec. III-A.1, the adopted coupler isolates the high frequency event-related components, but a decision protocol in still needed to decide on the fault's apparition. Accordingly, a threshold adapted to the testing environment is defined in order to avoid untimely triggers. Generally, it is manually set slightly above the ambient noise level. Thereafter, when the measured signal is above the threshold, the FOT is recorded.

Having recorded the signals, the arrival times of the acquired FOTs at each sensor shall be compared. Accordingly, the same time-base should be used for all detection systems. Notably, since the time dispersion of the internal clock of the oscilloscope is too high to ensure a correct synchronization between sensors, the time difference can be up to 10 μs, which correspond to an error in position of 2 km. It is

therefore necessary to use extremely stable clocks such as atomic clocks for each detection system in order to guarantee a good synchronization between each of them. We decided to use a GPS (Global Positioning System) chip coupled to a precision OCXO (Oven Controlled Crystal Oscillator) for improving the stability and accuracy of reference clocks. GPS transmits timing and position information from satellites and is cheaper than integrating a controlled atomic clock in the sensor, for the same results [23]. Eventually, this reduces the time difference by three orders of magnitude and ensures an error of localization in the range of two meters. As a result, FOTs accompanied with the occurrence of electrical events are captured and timestamped with a high precision by the acquisition system regardless their location and then saved on a text file in a windows folder. It is worthy to note that all modules (digitizer, timing and synchronization, GPS) are controlled by the the embedded controller drives through a LABVIEW application, leading to a user-friendly interface..

3) Communication Tool: To facilitate the process of handling, reading, and transferring event-related data, a remote control solution is implemented. We installed a communication tool based on a 4G network that enabled the communication of each data acquisition system with a central server. Therefore, once a FOT is detected, recorded and time-stamped at the level of each acquisition system, a scripted code implemented on the system checks in real-time if new data were added to the windows folder and if that was the case, it uses the 4G connection to the internet to send the data to a distant server.

B. FasTR fault location platform

The fault location platform comprises a server employed as a database for saving the recorded events and a computer unit to apply the FasTR algorithm for processing. All data arriving to the server are stored with meta information to ID them individually. As soon as new data arrives, a computer unit harnessing an executable version of the FasTR algorithm MATLAB code detailed in sec. II is launched for analysis. It interrogates the database and repatriates all data of the selected test and performs the calculus which can be done on any PC having the FasTR executable file and the right login info. We used in our tests a PC with an Intel Core i5 processor supporting Windows 7 operating system.

Once an event is detected, the corresponding information (fault position, location, and time of occurrence) is saved on a file and sent using the communication network back to the server. An immediate warning approach could be also implemented where an email or a text message could be sent to the nearest operation center and/or technician for urgent intervention.

IV. ON-SITE INSTALLATION

The testing process of any large-scale distribution network commences by a reconnaissance operation in coordination with the DSOs (distribution system operators). This allows mapping the network's topology (configuration, junctions, branch lengths, etc.), which will in turn be used to divide it into sub-networks. Once the area of interest within the large NUT is
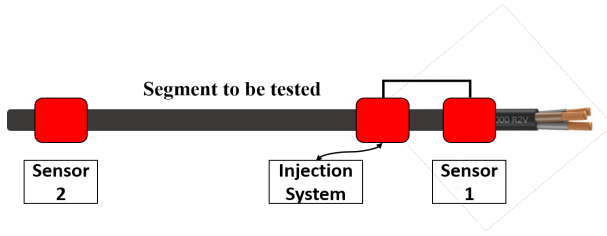
Fig. 3: The calibration process of each segment of the SNUT for estimating the speed of signal propagation.

defined, the sub-network to be tested (SNUT) is investigated so as to integrate its corresponding parameters in the simulation model of the fault location platform. The SNUT is further inspected to identify available stations in the area it resides and verify their compatibility in terms of accessibility and climatic conditions. Particularly, these are paramount factors when installing the measurement systems, where special attention shall be given to the ability of connecting the sensing units (couplers) on the desired cables/or phases, the proper functioning of the NI based acquisition systems (electricity plugs, convenient temperature, GPS coverage), and a reasonable 4G connection for the communication network. Subsequently, and depending on the size of the SNUT, the necessary number of sensors is determined.

The adopted sensing units are then coupled to the phases of interest on the SNUT to be monitored, and a calibration process is performed in parallel. In fact, the purpose of calibration is to return a good estimate of the propagation speed of signals along the segments of the SNUT. Particularly, this is important when dealing with non-homogeneous networks composed of segments having different cable types and consequently different propagation speeds. Fig. 3 illustrates the process of calibration which starts by generating at the input of sensor 1 a burst of 10 periods of a sinusoidal signal of frequency 100 kHz and amplitude 10 Vpp. In view of sensor's losses in addition to the attenuation and dispersion along the SNUT's segment, we expect to measure a very similar signal on sensor 1 and a somewhat distorted version of it with a delay on sensor 2. The time difference between the two measurements will give an estimate of the wave propagation conditions on the tested segment which is updated to the FasTR's simulation model. To reduce the bias and the risk of non-detection, we repeat the operation several times. Besides, this process not only estimates the velocity of propagation but also tests the electromagnetic continuity for the frequency bandwidth of interest.

The fault location setup is now ready to record any upcoming event and estimate its corresponding position and location.

V. Test Bed Description

A. Tested Network

The NUT is an underground medium-voltage (20 kV), three-phase supply network, made up of different types of coaxial cables in a village of Switzerland. The network is a mix of three types of cables where the majority are of XKDT type with an XLPE insulation material, while the rest are either

GKT cables with an EPR insulation, or Paper Pb cables with Paper insulation. It is a network in normal operation fed with electrical power. Fig. 4 demonstrates the main structure of the SNUT of interest which is part of a larger MV network, where lines represent the cables whereas blue boxes symbolize the substations that supply the low-voltage networks. The topology breaks down as follows:

1) Lines outside the plant: between substations B and C. These lines connect several other substations, including substation D, to which the plant is connected. These lines are of different lengths and types due to repair interventions accomplished over time.
2) Lines inside the plant: between substation D and the plant. The lengths indicated on the SNUT are approximate as precise lengths were not available.

The plant's substation contains a loop which is "normally open" but may be closed or opened according to user needs. Three sensing units have been all coupled to phase 3 of the SNUT at substations (A, B, and C), as demonstrated in Fig. 4. The selected positions presented the advantage of allowing surveillance over a good part of the plant's section of the network as well as close outside lines. The coverage scheme of the sensors is well presented in Fig. 4. It can be noted that other subnetworks exist beyond substations B and C, where event related signals propagating from corresponding lines can be still recorded and treated but with limited accuracy. The GPS antenna of the NI based data acquisition system was deployed in a way to ensure a good reception of the GPS signal.

At each substation there is an MV/LV (medium voltage-low voltage) transformer to step-down the power so as to be transmitted through the LV lines. The corresponding cables although connected to the substations, they are electrically isolated from a propagation point of view due to the galvanic isolation the transformers possess.

Thereupon, the network is modelled within the MATLAB-based fault location platform according to the prior-knowledge of the network topology and line/cable electrical parameters. This forms the anchor of the backward propagation phase of the FasTR algorithm so as to estimate the position and location of FOTs.

B. Fault Generating System

The pilot tests were carried out by an artificially triggering FOT generator which is composed of three elements:

- a disconnection system composed of a circuit breaker (CB) that allows to short-circuit one of the three phases of the SNUT's cable with the ground;
- an adjustable water resistor with values of 30 and 60 Ω;
- a spark igniter to give a better control over the instant of the arc occurrence.

The corresponding fault generator system has allowed the possibility of producing several types of faults depending on the combination of elements used. In our study we considered the following cases:
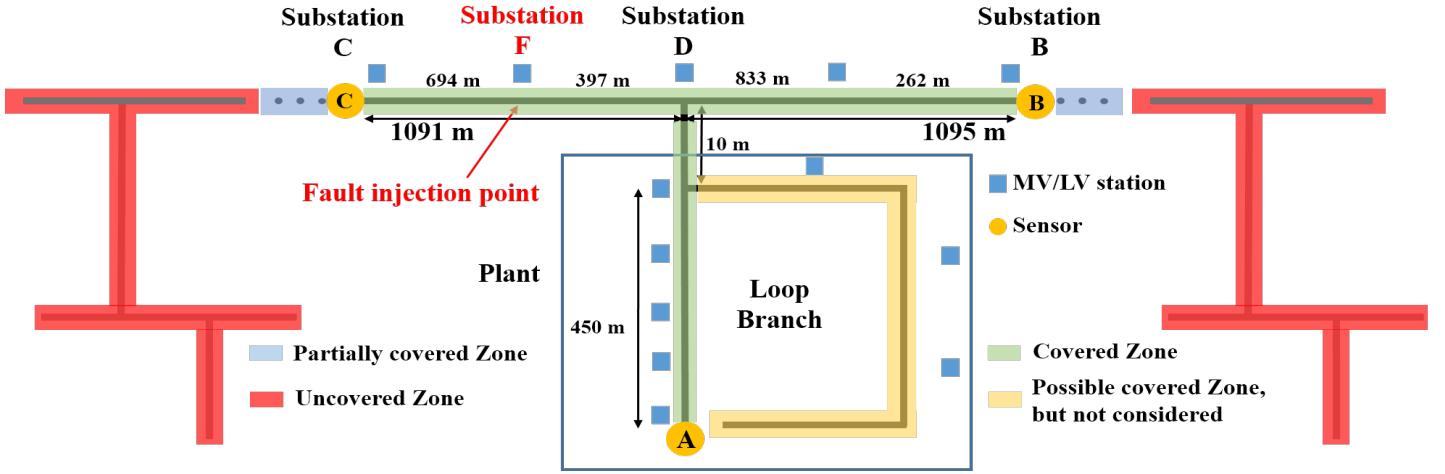
1) CB;
2) CB + spark igniter;

Fig. 4: The MV coaxial based network considered for the set of tests of the FasTR based fault location platform.

3) CB + 30 Ω;
4) CB + 60 Ω;
5) CB + spark igniter + 60 Ω.

The aforementioned combinations can be categorized into two main families: the first two are accounted as solid faults with an impedance ~ 0 Ω while the others are resistive faults. Particularly, a short-circuit solid fault leads to a sudden voltage drop to 0 V, thus generating a high-frequency FOT flowing through the network. The process is reversible so as to enable putting an end to the fault once the CB is returned to its off position. Notably, the same phenomenon occurs when the CB is released where the corresponding phase would be disconnected from the ground. The sudden rise in voltage generates a similar effect as before. The last fault assembly with a 60 Ω resistance is the most representative and encountered type of events in MV networks.

It is worthy to note that the control of the fault generating system has been manual and therefore temporally imprecise, that is to say the duration between two maneuvers (CB on and off) is subject to human precision which can be less than a second but much greater than five nanoseconds. However, this shall not pose any problem since the fault location is known and the fault location system can normally operate regardless the start time of the maneuver. On the other hand, the duration between 2 maneuvers must remain relatively short (a few seconds) so as not to exceed the time required to trigger the network security devices which would cut-off the entire sector.

C. Fault position

The fault generator system was put on a truck so that it could be transportable and easily replaceable. Several considerations were taken into account before connecting it to the NUT. First of all, it is necessary to ensure the presence of a free connection on the network so that the fault generator could be branched. In addition, since the truck and the necessary safety perimeters could occupy a considerable space on the public roadway, it must be located in an accessible and sufficiently spacious area. Finally and more importantly, it is necessary to position the fault-triggering system on a location well-covered by the sensing units, i.e. to say within the green coverage zone of the SNUT as shown in Fig. 4. With all these in mind, substation F formed a perfect match with the aforesaid conditions and was chosen to serve as the location where the fault generator will be installed. Accordingly, the truck containing the fault generator was transported to substation F which is 694 m away from substation C, and connection cables were employed so as to connect the system to the phase monitored by the sensors. Meanwhile, thanks to the 4G remote connection, operators took control of the sensing units and ensured that they are functional and correctly adjusted.
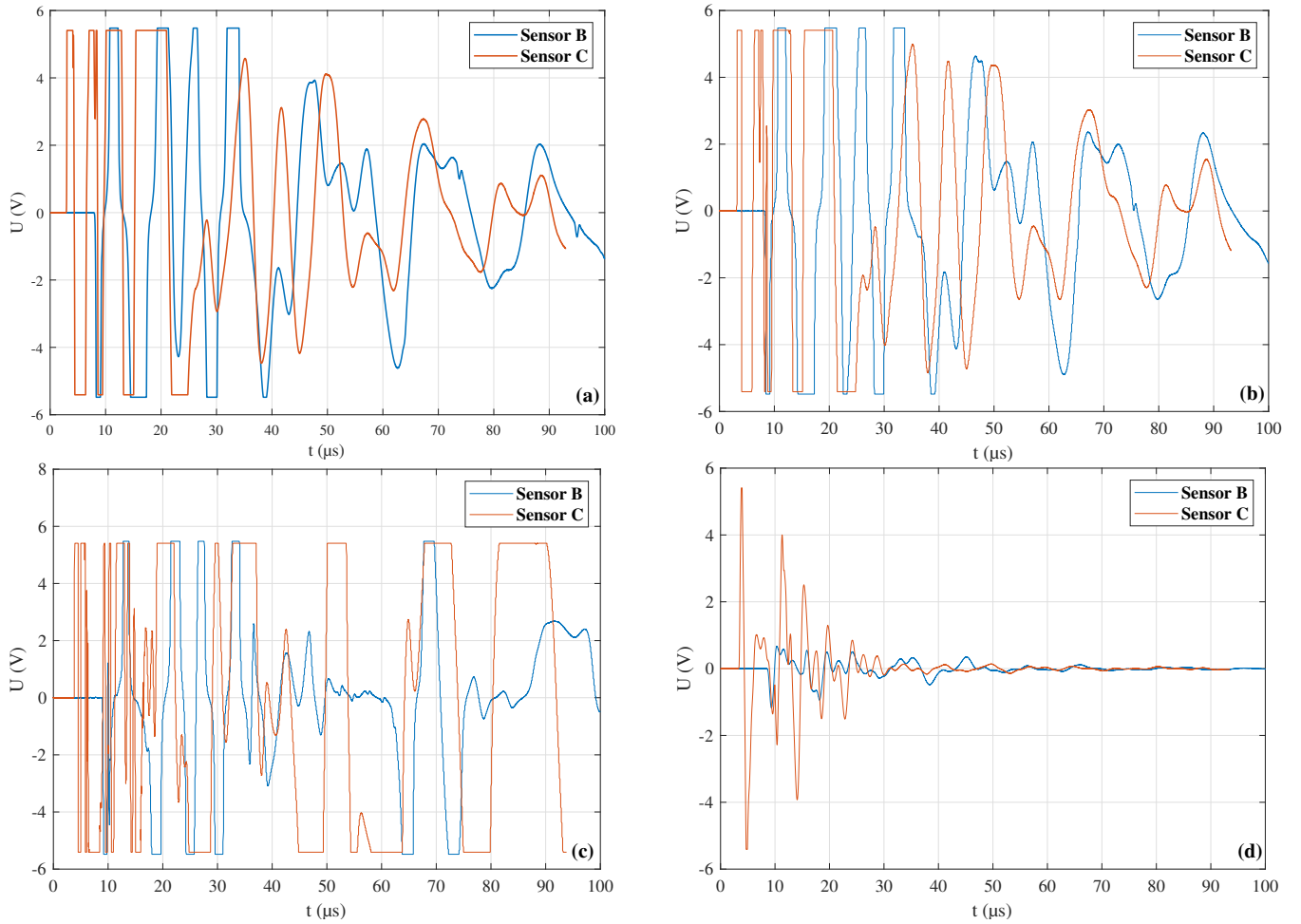
VI. NETWORK FIELD TESTING

With the system installed on the on-line network, the FasTR-based fault monitoring setup was tested on the set of manual-triggered faults presented in sec. V-B in order to assess its performance. Faults were generated, recorded, transferred and treated within the interval of 30 min on March 2019.

A. Triggered Fault Events

Considering the different fault types afforded by the elements' combinations that the fault generating system enables, several tests have been accomplished on each of the following triggered events.

1) Circuit breaker: The CB alone has been connected between phase 3 (the phase monitored by the sensing units) and the ground at substation F. An operator manually pushes the activation switch, connecting the phase with the ground and approximately 1 s later pushes the release button to open the circuit and stop the fault. The sudden connection to the ground creates a distortion of the three-phased voltage and a high-frequency FOT propagates along the NUT. The sensing units capture the FOT and the measurement setup transmits the time-stamped data to the remote server for post-processing. This procedure has been repeated twice, first to verify the proper functioning of the network protection modules and on the other hand to verify the proper functioning of the measurement chain on the sensors.

Fig. 5: Amplitude of the FOTs' voltage as measured by sensors B and C for the faults triggered by: (a) CB and 30 Ω resistance, (b) CB and 60 Ω resistance, (c) CB with the spark ignitor, and (d) CB with the spark ignitor and a 60 Ω resistance.

Sensors B & C identified and recorded the FOT, whereas the threshold-triggering criterion of A captured nothing abnormal.

2) CB and water resistance: Two successive tests were made with the CB and the water resistor. During the first test, the resistance was set to a value of 30 Ω while during the second test it was set to 60 Ω. The value of the resistance desired was set by adjusting the level of water. Again, the events were detected and recorded by the sensors B & C only.

3) CB with the spark ignitor: A test was then carried out by removing the water resistor and connecting the spark ignitor in series with the CB. This was intended to reset the fault at each half-period of the 50 Hz fundamental power signal. These kind of events are representative of breakdowns which appear in a degrading MV network. The resulting generated events were successfully recorded at sensors B & C.

4) CB with the spark ignitor and the water resistance: The last test carried out included all components of the fault generating system. The water resistor has been set to 60 Ω so as to test the most difficult configuration that can be detected theoretically. During this test, sensors at substations B & C were capable of detecting and recording events when the fault was activated.

B. Test Results

Figs. 5 (a), (b), (c), and (d) depict the FOTs measured at the level of sensors B and C for the faults triggered as a result of the CB with the 30 Ω resistance (scenario 1), the CB with the 60 Ω resistance (scenario 2), the CB with the spark ignitor (scenario 3), and the the CB with the spark ignitor and a 60 Ω resistance (scenario 4) respectively. It can be well noted that a powerful transient signal with its corresponding timestamp has been successfully recorded by each of the two sensors. Besides, despite the lengthy NUT accompanied with considerable attenuation, the FOTs have been strong enough to lead to a quick saturation of the oscilloscope as the curves attest. They traverse the whole network and "rebound" on all nodes and extremities several times before fading away.

The voltage levels measured by the events generated by the CB with the water resistor are very similar between the case of the 30 Ω and that of the 60 Ω. The saturation obtained made it difficult to see a real difference, as one would expect. However, scenario 3 hosting the spark ignitor with the CB produced a high voltage level which is obviously justified since the triggered event is close to that of a short circuit. The combination of all elements in fault scenario 4, in the most restrictive configuration, has also generated a detectable
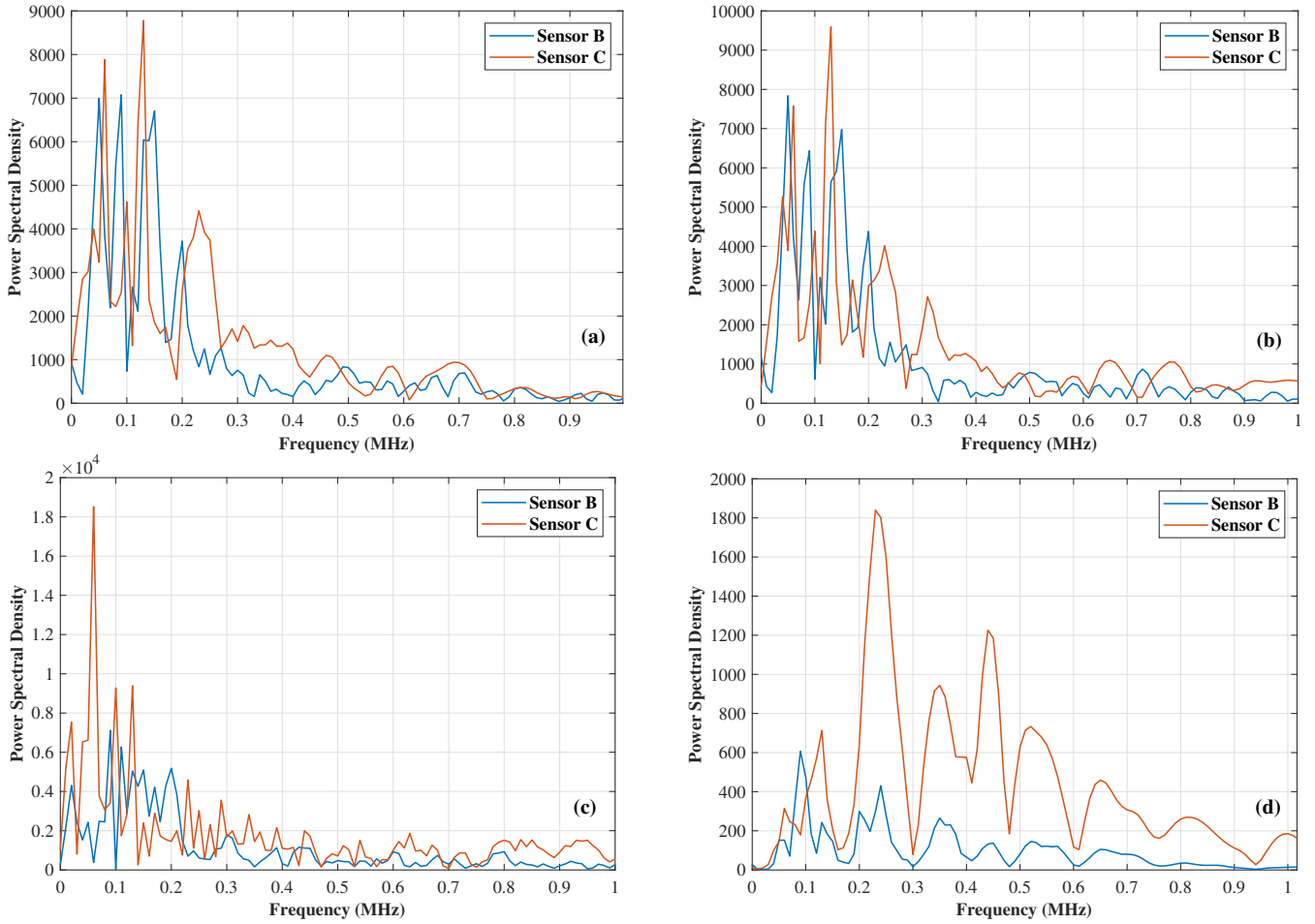
Fig. 6: Spectra of the FOTs as measured by sensors B and C for the faults triggered by: (a) CB and 30 Ω resistance, (b) CB and 60 Ω resistance, (c) CB with the spark ignitor, and (d) CB with the spark ignitor and a 60 Ω resistance.

TABLE I: Results obtained after applying FasTR algorithm on the measured data of the pilot tests.

	Actual triggered		Retrieved estimated		
Test	Phase	Location	Phase	Location	Time
Scenario 1	L_3	694 m	L_3	667 m	55 s
Scenario 2	L_3	694 m	L_3	667 m	57 s
Scenario 3	L_3	694 m	L_3	643 m	54 s
Scenario 4	L_3	694 m	L_3	640 m	60 s

event, although it presented a much lower power level than the previous cases. As mentioned earlier, it remains true that only the presence of the spark ignitor allows control over the voltage level when the fault is triggered.

Table I reports the results obtained after applying FasTR algorithm on the received data. They first prove that the correct phase that has been triggered is correctly identified in all scenarios. More importantly, a good estimate of the fault's position has been returned with an average error of no more than 2% of the total SNUT's length. The computation time ranges between 50 to 70 s in all tested scenarios using the Intel I5 2.3 GHz processor, a remarkable feature emphasizing an excellent resolution within the scope of affording an on-the-fly analysis of transient events.

C. Transient Spectral Analysis

The spectra of the measured FOTs corresponding to the tested faults are presented in Figs. 6 (a), (b), (c), and (d). Three different spectral responses can be differentiated. The first corresponds to the fault scenarios 1& 2 where the CB was connected to two resistances provided by the water resistor. The spectra of the recorded FOTs are similar with peaks around 60 kHz, 90 kHz and 120 kHz and a lower peak at 240 kHz. It should be kept in mind that saturation comes here to disturb the responses since it also generates visible harmonics on the studied band.

With fault scenario 3 where the spark ignitor alone is connected to the CB, the frequency response is concentrated mainly around a single peak around 60 kHz for the signal picked up by sensor C. Strangely, this harmonic is absent from the signal picked up by sensor B.

Finally, the measurements recorded as a result of event scenario 4 where all elements of the fault generation system are connected seems to be very different from the other spectra. Particularly, the signal measured by sensor C is quite rich in harmonics since it has several high peaks, this time around higher frequencies (230 kHz, 350 kHz, 440 kHz, and 530 kHz). Nevertheless, sensor B collected a FOT with a much

weaker response and distorted high harmonics. The network accordingly has a filtering effect.

VII. PERFORMANCE ANALYSIS

A. Transient Signal Amplitude

It might be difficult to give grounds for the high voltage levels obtained as Fig. 5 shows. It seems that the shield currents generated during the maneuvers are very high. Additionally, a phenomenon of self-maintenance of the coil currents in the used inductive couplers might have occurred. Characterization tests have shown the later aspect plays an important role in the shape of the signals obtained, in particular the presence of positive/negative alternations. In fact, since we do not control the triggering moments of the fault generation system during the 50 Hz signal period, we may compare two very different trigger levels for which the current generated with the value 60 Ω, for example, is much stronger at this time than those obtained with the value 30 Ω. The fact remains that the signals are far above the noise level and can be exploited by the FasTR method. The resistance value, even in the presence of the spark gap does not seem to be a concern with regard to the objective of detecting representative faults.

B. Network Coverage

The signals captured by the sensing units and sent to the data acquisition system have shown that sensor A wasn't capable of detecting any high-frequency signal during the tests. This might be returned to several hypotheses that can explain the observation. First, sensor A was located at an extremity end of its branch, which is terminated by an open circuit, whereas sensors B and C were coupled to the SNUT at substations where the network extends. No current should be going through the insulation shield at this point, and thus transients cannot be detected with such a positioning. Furthermore, this branch of the network is located inside the plant where it is possible that the connection to the external network can behave as a low-pass filter, thus blocking any transient signals. Nevertheless, FasTR algorithm was still capable of operating with incomplete or missing data from sensor A. Although, it reduces the portion of the network where a position can be pinpointed, but as the source of the transients is on the direct path between sensors B and C, the algorithm can still converge to an exact solution. Accordingly, one can conclude that the presence of sensors covering the direct path where an event occurs is enough to enable locating its position.

C. Location Accuracy

The fault location platform has provided a position accuracy ranging from a minimum error of 27 m and maximum of 54 m. Apparently, it is higher than the theoretical bias introduced by the oscilloscope sampling rate and the use of GPS synchronization which should have been summed up to 5 m approximately. However, such a difference can be returned to the rough estimate of the propagation speed in the SNUT. In fact, the latter has been assumed constant in the numerical model of the post-processing algorithm although the monitored network was composed of at least three different types of underground MV cables having different phase velocities. Particularly, an error of 1% in the wave celerity can lead to a 25 m positioning error. Notwithstanding, with a better method of precise calibration and a more accurate GPS system, the result should be greatly improved. Nevertheless, such a result is still satisfying for locating powerful transient signals'source locations.

VIII. CONCLUSION

This paper has demonstrated the capacity of an on-deck portable system based on the tenets of FasTR method to locate transient faults in complex power networks during their normal operation. The contactless sensing inductive couplers and the compact size of the data acquisition system facilitate their on demand deployment for monitoring networks at risk. Thanks to a well-established user friendly platform integrating a built-in communication network and a distant data server, it also became possible to remotely control the system and send measured data to the central server without human intervention. More importantly, a warning alarm could be broadcasted to local operators once an event occurs in no more than a handful minutes.

Pilot tests were performed on a 2.5 km MV underground network in Switzerland by short-circuiting to the ground a phase of the power supply system. Particularly, the tested cases covered two main categories of faults: solid short-circuits and resistive faults. The later are good representatives of small shutdown precursors, as they limit the power of FOT signals flowing through the network. Significantly, the proposed monitoring system successfully detected the transient faults through its distributed sensors, and, thanks to a high-quality time synchronization combined with the FasTR method, it was able to locate the source location with good reliability. Furthermore, the fact that good results were obtained with missing data from one of the sensors enhanced the notion of the method's applicability with a reduced number of sensors.

It is important to note that FasTR algorithm did not give a unique position value for all tested faults, although they were generated from the same point of the network. The location error obtained had an average in the order of 40 m, which is beyond the margins of tolerance associated with measurement inaccuracies and time stamping ($\approx$ 4 m). This forced to question the performance of the calibration process and the precision of the GPS system, which once rectified shall correct the bias from the incorrect estimation of wave celerity in the network and thus reduce the deviation from the eventual positions.

The procured promising outcome has therefore demonstrated the value of the FasTR-based fault location system. This has proven its ability to properly detect representative faults under control, which is a remarkable result in the domain of fault location in underground MV networks. The principle of the measurement/processing chain has been fully demonstrated, despite the residual discrepancies noted on the location. Better knowledge of the networks, in particular by estimating the phase velocities by section, will make it

possible to correctly assess the performance of the system and to improve the fluidity of the processing chain, taking into account the generality of the cases that will be encountered later. This procedure with the corresponding platform has been kept in operation on the same network on the course of a long period listening campaign to deal with natural-triggered events. The obtained results will be further presented.

ACKNOWLEDGMENT

REFERENCES

[1] R. A. Verzijlbergh, M. O. Grond, Z. Lukszo, J. G. Slootweg, and M .D. Ilic, "Network impacts and cost savings of controlled EV charging," in *IEEE Transactions on Smart Grid*, vol. 3, no. 3, pp. 1203–1212, 2012.

[2] S. Bumby, E. Druzhinina, R. Feraldi, D. Werthmann, R. Geyer, and J. Sahl, "Life cycle assessment of overhead and underground primary power distribution," in *Environmental science & technology*, vol. 44, no. 14, pp. 5587–5593, 2010.

[3] J. Lassila, T. Kaipia, J. Haakana, J. Partanen, and K. Koivuranta, "Potential and strategic role of power electronics in electricity distribution systems," in *CIRED 20th International Conference and Exhibition on Electricity Distribution-Part 1*, pp. 1–5, 2009.

[4] C. Furse, M. Kafal, R. Razzaghi, and Y. J. Shin, "Fault Diagnosis for Electrical Systems and Power Networks: A Review," in *IEEE Sensors Journal*, April 2020.

[5] P. F. Gale, P. A. Crossley, X. Bingyin, G. Yaozhong, B. J. Cory, and J. R. G. Barker, "Fault location based on travelling waves," in *in Proc. 5th Int. Conf. Develop. Power Syst. Protection*, Mar. 1993, pp. 54–59.

[6] G. B. Ancell and N. C. Pahalawaththa, "Maximum likelihood estimation of fault location on transmission lines using travelling waves," in *IEEE Trans. Power Del.*, vol. 9, no. 2, pp. 680–689, Apr. 1994.

[7] A. O. Ibe and B. J. Cory, "A travelling wave-based fault locator for two- and three-terminal networks," in *IEEE Trans. Power Del.*, vol. 1, no. 2, pp. 283–288, Apr. 1986.

[8] Z. Q. Bo, G. Weller, and M. A. Redfern, "Accurate fault location technique for distribution system using fault-generated high-frequency transient voltage signals," in *IEEE Proceedings-Generation, Transmission and Distribution*, vol. 146, no. 1, pp. 73–79, Jan. 1999.

[9] M. Fink, "Time reversal of ultrasonic fields. I. Basic principles," in *IEEE transactions on ultrasonics, ferroelectrics, and frequency control*, vol. 39, no. 5, pp. 555–566, Sep. 1992.

[10] M. Kafal, R. Razzaghi, A. Cozza, F. Auzanneau, and W. Ben Hassen, " A review on the application of the time reversal theory to wire network and power system diagnosis," in *IEEE International Instrumentation and Measurement Technology Conference (I2MTC)*, May 2019.

[11] M. Kafal, A. Cozza, and L. Pichon, "Locating multiple soft faults in wire networks using an alternative DORT implementation," in *IEEE Transactions on Instrumentation and Measurement*, vol. 65, no. 2, pp. 399–406, 2015.

[12] M. Kafal, A. Cozza, and L. Pichon, "Locating Faults With High Resolution Using Single-Frequency TR-MUSIC Processing," in *IEEE Transactions on Instrumentation and Measurement*, vol. 65, no. 10, pp. 2342–2348, 2016.

[13] R. Razzaghi, G. Lugrin, H. Manesh, C. Romero, M. Paolone, and F. Rachidi, "An efficient method based on the electromagnetic time reversal to locate faults in power networks," in *IEEE Trans. Power Del.*, vol. 28, no. 3, pp. 1663–1673, Jul. 2013.

[14] S. Y. He et al., "Norm Criteria in the Electromagnetic Time Reversal Technique for Fault Location in Transmission Lines," in *IEEE Transactions on Electromagnetic Compatibility*, vol. 60, no. 5, pp. 1240–1248, Oct. 2018.

[15] Z. Wang, R. Razzaghi, M. Paolone, and F. Rachidi, "Electromagnetic time reversal applied to fault location: On the properties of back-injected signals," in *in 20th Power Systems Computation Conference*, PSCC 2018.

[16] S. Y. He, A. Cozza, and Y. Xie, "Electromagnetic Time Reversal as a Correlation Estimator: Improved Metrics and Design Criteria for Fault Location in Power Grids," in *IEEE Transactions on Electromagnetic Compatibility*, pp. 1–14, Jun. 2019.

[17] Z. Wang et al., "A Full-Scale Experimental Validation of Electromagnetic Time Reversal Applied to Locate Disturbances in Overhead Power Distribution Lines," in *IEEE Transactions on EMC*, vol. 60, no. 5, pp. 1562–1570, 2018.

[18] Z. Wang, R. Razzaghi, M. Paolone, and F. Rachidi, "Time reversal applied to fault location in power networks: Pilot test results and analyses," in *International Journal of Electrical Power and Energy Systems*, vol. 114, Jan. 2020

[19] M. Kafal, N. Gregis, J. Benoit, and N. Ravot, "An Effective Method Based on Time Reversal and Optimization Techniques for Locating Faults on Power Grids," in *IEEE Sensors Journal*, June 2020.

[20] Z. Michalewicz, *Genetic algorithms+ data structures= evolution programs*. Springer Science & Business Media, 2013.

[21] J. C. Eidson, "Measurement, control, and communication using IEEE 1588," in *Springer Science & Business Media*, 2006.

[22] G. S. Antonova, et al., " Standard profile for use of IEEE std 1588-2008 precision time protocol (PTP) in power system applications," in *66th IEEE Annual Conference for Protective Relay Engineers*, pp. 322–336, 2013.

[23] P. C. J. M. Van der Wielen, "On-line detection and location of partial discharges in medium-voltage power cables," in *Electrical Power Systems (EPS) Group*, 2005.